

# Exceptional-Point Lineage and the Stability Architecture of Physical Reality: Symmetrical Convergence Across Quantum and Cosmic Scales

Nate Christensen

SymC Universe Project, Missouri, USA

NateChristensen@SymCUnciverse.com

09 February 2026

## Abstract

Physical reality is organized by structural boundaries. The dimensionless damping ratio  $\chi \equiv \gamma/(2|\omega|)$  defines a stability architecture in which the critical threshold  $\chi = 1$  marks a second-order non-Hermitian Exceptional Point (EP). A parameter-free identity is derived linking cosmic acceleration to critical damping,  $\chi_\delta = 1 \iff q = 0$ , indicating a structural constraint on the timing of dark energy dominance. The result is structural rather than causal: it follows from the form of the growth and Friedmann equations within flat  $\Lambda$ CDM, independent of any microscopic model for dark energy. This stability condition propagates through a substrate inheritance relation, whereby emergent modes inherit EP structure from vacuum precursors. Within this framework, the observed particle distribution is consistent with stability organization: long-lived matter occupies localized stability basins at  $\chi \ll 1$ , while short-lived excitations cluster near the  $\chi = 1$  interface. The framework replaces ad hoc parameter tuning with a stability-based classification principle.

## 1 Boundary Structure in Dissipative Dynamics

Physics is organized by boundaries. The speed of light  $c$  limits information propagation, and Planck's constant  $\hbar$  bounds measurement precision. The dimensionless ratio

$$\chi \equiv \frac{\gamma}{2|\omega|} \tag{1}$$

plays an analogous role in dynamical stability.

At  $\chi = 1$ , the generator of dynamics becomes defective and the impulse response transitions to

$$h(t) = te^{-|\omega|t}, \tag{2}$$

defining a second-order non-Hermitian exceptional point (EP2) [3, 12, 13].

Quadratic eigenproblems for linear response arise across classical dissipative modes, retarded propagators in open quantum field theory, and cosmological growth dynamics [5, 7, 10, 17]. In each case, the exceptional-point kernel appears when the damping rate matches twice the characteristic frequency,  $\chi = \gamma/(2|\omega|) = 1$ . Markovian open-system generators of Lindblad type can realize the

same EP2 structure in suitable reduced response channels or effective mode equations (Supplementary Section 1) [11, 14], but the EP condition is asserted here at the level of the shared quadratic response structure.

For representative linear response channels with Gaussian noise and finite bandwidth, an information-efficiency functional  $\eta(\chi) \equiv I(\chi)/\Sigma(\chi)$  admits a strict local maximum in a narrow neighborhood of  $\chi = 1$  under standard smoothness conditions (Supplementary Section 2). This supports the interpretation of near-critical damping as a robust operating point balancing responsiveness against dissipation in common model classes.

A strict local maximum at  $\chi = 1$  follows if  $\eta(\chi)$  is twice differentiable in a neighborhood of  $\chi = 1$ ,  $\eta'(1) = 0$ , and  $\eta''(1) < 0$ . The Gaussian-channel examples provide an explicit realization of these conditions.

Most significantly, the onset of cosmic acceleration ( $q = 0$ ) is mathematically identical to the structure growth field reaching critical damping ( $\chi_\delta = 1$ ), providing a structural explanation for the timing of late-time acceleration without fine-tuning.

## 2 Exceptional-Point Kernel and Efficiency Extremum

For a representative linear mode whose observable response obeys a second-order dissipative equation:

$$\ddot{x} + \gamma\dot{x} + \omega^2x = 0, \quad (3)$$

the characteristic discriminant

$$\Delta = \gamma^2 - 4\omega^2 = 4\omega^2(\chi^2 - 1) \quad (4)$$

vanishes at  $\chi = 1$ , yielding coalesced roots  $\lambda_{\pm} = -|\omega|$  and the EP2 impulse kernel (2) [13]. Such quadratic response structures appear directly in classical linear-response theory and in retarded propagators of dissipative quantum field theory [5]. Lindblad-form Markovian dynamics can realize the same EP2 kernel in appropriate effective response channels; the mapping and its scope are given explicitly in Supplementary Section 1 [11, 14].

An identical structure arises in dissipative quantum field theory. For a scalar mode with retarded propagator

$$G_R(\Omega) = \frac{1}{-\Omega^2 - i\gamma\Omega + \omega^2}, \quad (5)$$

the poles

$$\Omega_{\pm} = -\frac{i\gamma}{2} \pm \sqrt{\omega^2 - \frac{\gamma^2}{4}} \quad (6)$$

coalesce at  $\gamma = 2|\omega|$ , reproducing the same EP2 kernel [5].

The information-efficiency functional

$$\eta(\chi) \equiv \frac{I(\chi)}{\Sigma(\chi)} \quad (7)$$

exhibits a strict local maximum at  $\chi = 1$  in Gaussian channel models (Supplementary Section 2). This identifies  $\chi = 1$  as a recurrent structural boundary in systems that simultaneously admit responsiveness and stability.

Physically,  $\chi < 1$  corresponds to persistent ringing, while  $\chi > 1$  sacrifices responsiveness. Realistic constraints broaden the optimum to a narrow window near criticality [15]. Figure 1 visualizes this dual structure as an exceptional-point manifold separating overdamped and underdamped regimes.

## Non-Hermitian Topology of the Vacuum-to-Matter Interface

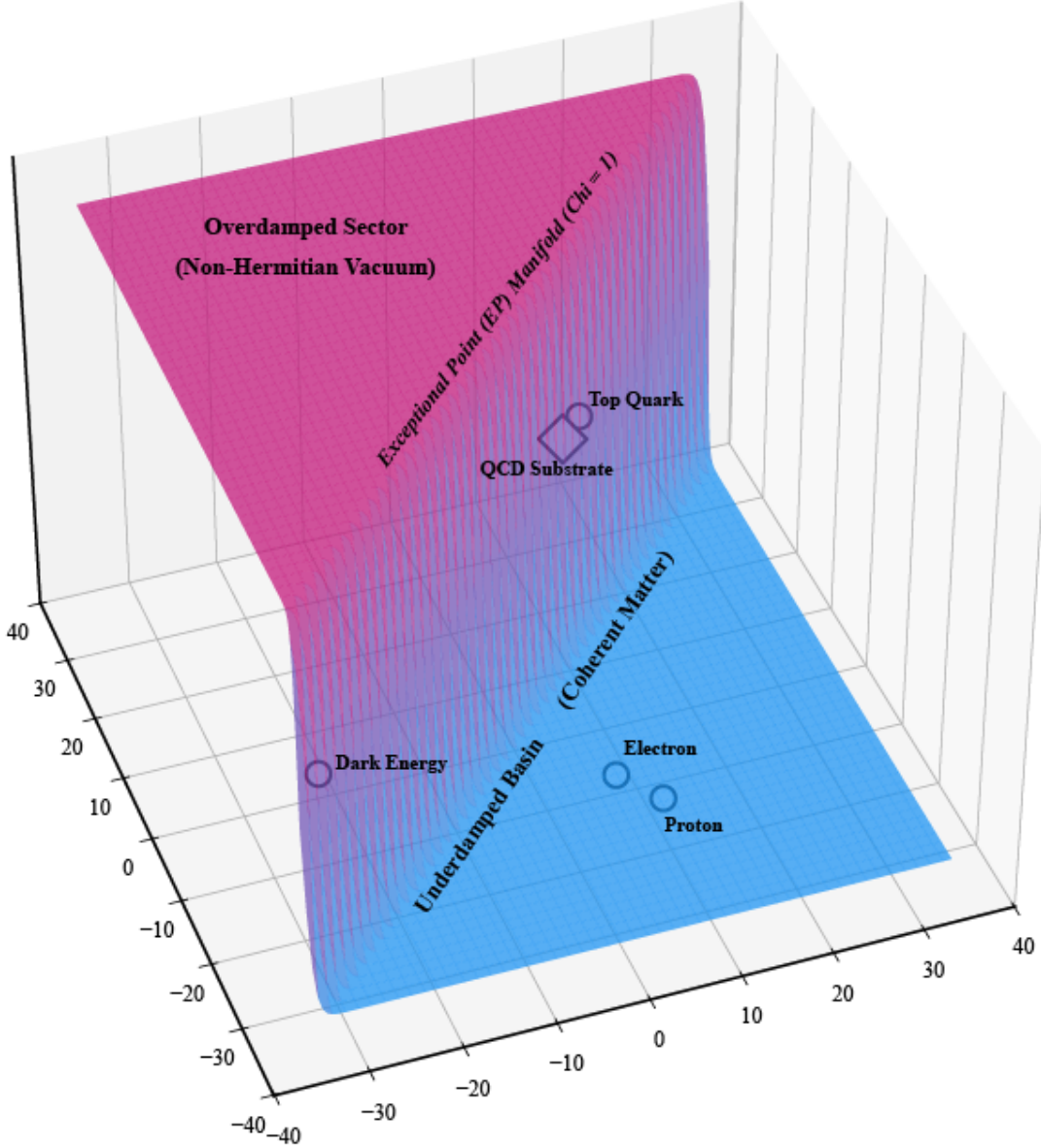


Figure 1: **Topological structure of the stability manifold.** Three-dimensional visualization in  $(\log_{10} \omega, \log_{10} \Gamma, \chi)$  space where  $\chi = \Gamma/(2\omega)$  is the dimensionless damping ratio. The colored surface represents the exceptional point (EP) manifold at  $\chi = 1$ , separating overdamped ( $\chi > 1$ , magenta) and underdamped ( $\chi < 1$ , blue) dynamical regimes. Representative systems illustrate an ordering by observed stability index: vacuum-lineage processes appear near the critical line, while long-lived excitations lie deep in the underdamped basin. The schematic language is classificatory and does not assert a microscopic pathway. Vertical projection lines connect the 3D topology to the empirical validation plane (Figure 3).

## Structural interpretation

The exceptional-point boundary at  $\chi = 1$  is not interpreted as a dynamical attractor. Rather, it serves as a structural separatrix where impulse response transitions from oscillatory to monotone decay. In representative dissipative channels (second-order systems with Gaussian noise and finite bandwidth), the information-efficiency functional  $\eta(\chi)$  admits a strict local maximum at  $\chi = 1$ . Departures from  $\chi \approx 1$  incur complementary penalties:  $\chi < 1$  produces persistent ringing that degrades signal fidelity under finite bandwidth, while  $\chi > 1$  produces slow relaxation that suppresses information throughput for fixed dissipation. The framework interprets near-critical operation as a robust efficiency extremum, consistent with observed system clustering in the range  $0.8 \lesssim \chi \lesssim 1.0$ .

### 3 Cosmic Crossing: $\chi_\delta = 1 \iff q = 0$

Linear density perturbations satisfy

$$\ddot{\delta} + 2H\dot{\delta} - 4\pi G\rho_m\delta = 0 \quad (8)$$

[10, 17], yielding

$$\chi_\delta = \frac{H}{\sqrt{4\pi G\rho_m}}. \quad (9)$$

In flat  $\Lambda$ CDM, the deceleration parameter

$$q = \frac{1}{2}\Omega_m - \Omega_\Lambda \quad (10)$$

vanishes at  $\Omega_m = 2/3$ . The Friedmann equations then give

$$H^2 = 4\pi G\rho_m, \quad (11)$$

implying the exact identity

$$\chi_\delta = 1 \iff q = 0. \quad (12)$$

The same structure appears at the generator level by rewriting the growth equation as a first-order system,

$$\frac{d}{dt} \begin{pmatrix} \delta \\ \dot{\delta} \end{pmatrix} = \mathcal{L}_\delta \begin{pmatrix} \delta \\ \dot{\delta} \end{pmatrix}, \quad \mathcal{L}_\delta = \begin{pmatrix} 0 & 1 \\ 4\pi G\rho_m & -2H \end{pmatrix}. \quad (13)$$

The eigenvalues of  $\mathcal{L}_\delta$  are

$$\lambda_\pm = -H \pm \sqrt{H^2 - 4\pi G\rho_m}, \quad (14)$$

which coalesce precisely when  $H^2 = 4\pi G\rho_m$ , equivalent to  $\chi_\delta = 1$ .

This parameter-free identity links cosmic acceleration onset to critical damping of structure growth.

**Scope of the identity.** Equation (12) holds *exactly* for spatially flat  $\Lambda$ CDM. In non-flat cosmologies or in  $w$ CDM with  $w \neq -1$ , the synchronization between the acceleration transition and the critical-damping crossing is no longer exact, but the stability crossing  $\chi_\delta = 1$  remains well-defined and shifts to a nearby redshift. This makes departures from  $\Lambda$ CDM testable as measurable offsets between the  $q = 0$  and  $\chi_\delta = 1$  transitions. Figure 2 demonstrates this synchronization.

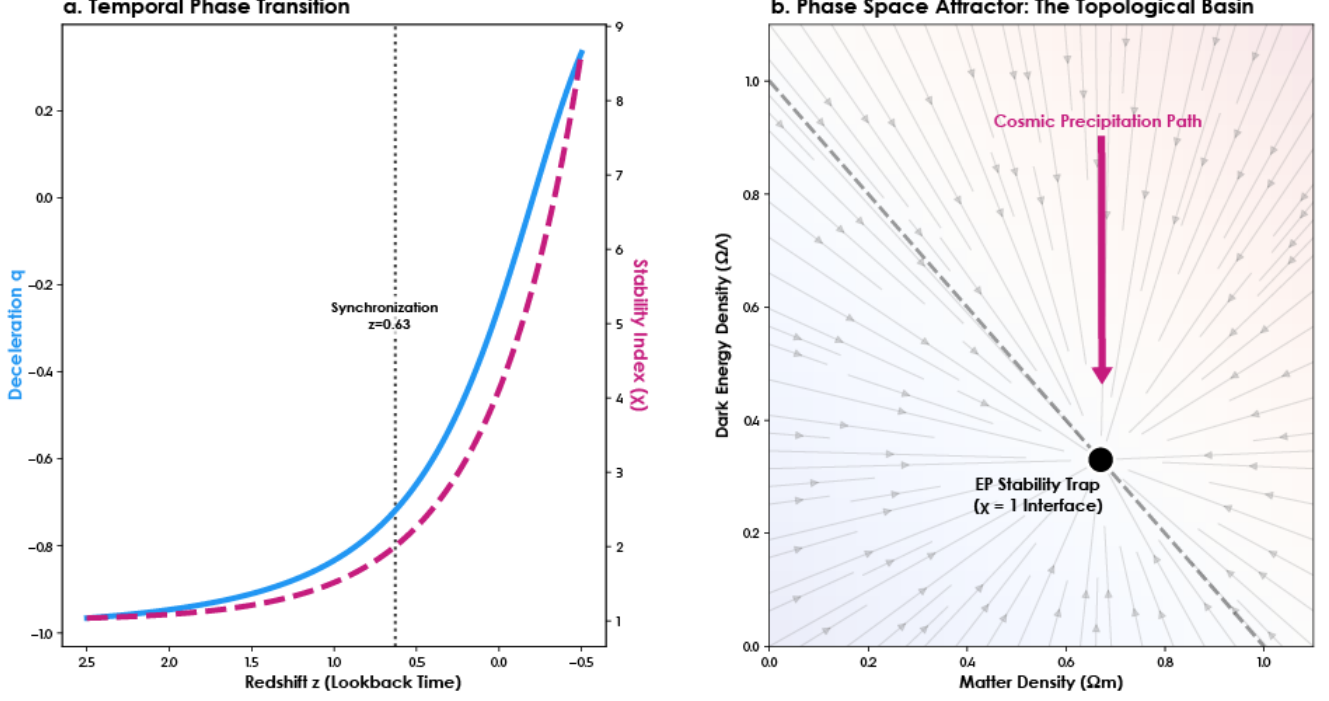


Figure 2: **Cosmological synchronization of critical damping and acceleration onset.** (a) Temporal evolution showing the deceleration parameter  $q(z)$  (blue) and stability index  $\chi_\delta(z)$  (magenta dashed) as functions of redshift. The curves intersect at the redshift where both  $q = 0$  and  $\chi_\delta = 1$  simultaneously. (b) Phase space representation with matter density  $\Omega_m$  and dark energy density  $\Omega_\Lambda$  as coordinates. The cosmic trajectory is shown for the concordance values  $\Omega_m \approx 0.3$  and  $\Omega_\Lambda \approx 0.7$ .

This result is parameter-free within flat  $\Lambda$ CDM and independent of any cosmological origin model [18–20].

## 4 Robustness Under Interactions and Memory

In weakly interacting  $\lambda\phi^4$  theory, renormalization-group flow yields

$$\frac{d\chi}{d\ell} = (a_\gamma - a_\omega)\lambda\chi, \quad (15)$$

so that  $\chi$  remains marginal when  $a_\gamma \approx a_\omega$  [21]. One-loop calculations show  $|\Delta\chi| < 1\%$  over multiple decades [24].

Finite-memory baths with kernel  $K(t) = \gamma_0 e^{-t/\tau}$  yield an effective damping

$$\gamma_{\text{eff}}(\omega) = \frac{\gamma_0}{1 + (\omega\tau)^2}, \quad (16)$$

broadening but not destroying the critical boundary [5]. The physically realized damping ratio in such environments is therefore

$$\chi_{\text{phys}}(\omega) \equiv \frac{\gamma_{\text{eff}}(\omega)}{2\omega} = Z(\omega\tau)\chi_{\text{bare}}, \quad Z(\omega\tau) = \frac{1}{1 + (\omega\tau)^2} < 1, \quad (17)$$

so that the exceptional point at  $\chi_{\text{bare}} = 1$  corresponds to a downward-shifted operating point when expressed in terms of effective rates.

## 5 Substrate Inheritance as a Structural Relation

Let  $\{\phi_k\}$  denote substrate modes with frequencies  $\Omega_k$  and damping  $\Gamma_k$ . Any emergent mode  $\psi = \sum_k c_k \phi_k$  inherits effective parameters

$$\Omega_\psi^2 = \sum_k |c_k|^2 \Omega_k^2, \quad \Gamma_\psi = \sum_k |c_k|^2 \Gamma_k. \quad (18)$$

The resulting damping ratio is

$$\chi_\psi = \frac{\Gamma_\psi}{2\sqrt{\Omega_\psi^2}}. \quad (19)$$

To make the overlap structure intrinsic, define the stabilized substrate subspace  $\mathcal{H}_s$  and the corresponding orthogonal projector

$$\mathcal{P}_s \equiv \sum_{i \in s} |\phi_i\rangle\langle\phi_i|. \quad (20)$$

For any proto-mode  $|\psi_{\text{proto}}\rangle$ , the substrate overlap is defined geometrically as

$$\epsilon_\psi \equiv \|\mathcal{P}_s|\psi_{\text{proto}}\rangle\|^2 = \langle\psi_{\text{proto}}|\mathcal{P}_s|\psi_{\text{proto}}\rangle. \quad (21)$$

In a substrate eigenbasis this reduces to  $\epsilon_\psi = \sum_{i \in s} |\langle\phi_i|\psi_{\text{proto}}\rangle|^2$ .

Empirically, long-lived particles occupy the underdamped basin  $\chi \ll 1$ , while short-lived resonances cluster near  $\chi \approx 1$ . This distribution is shown in Figure 3.

## The Mechanical Lineage of Matter

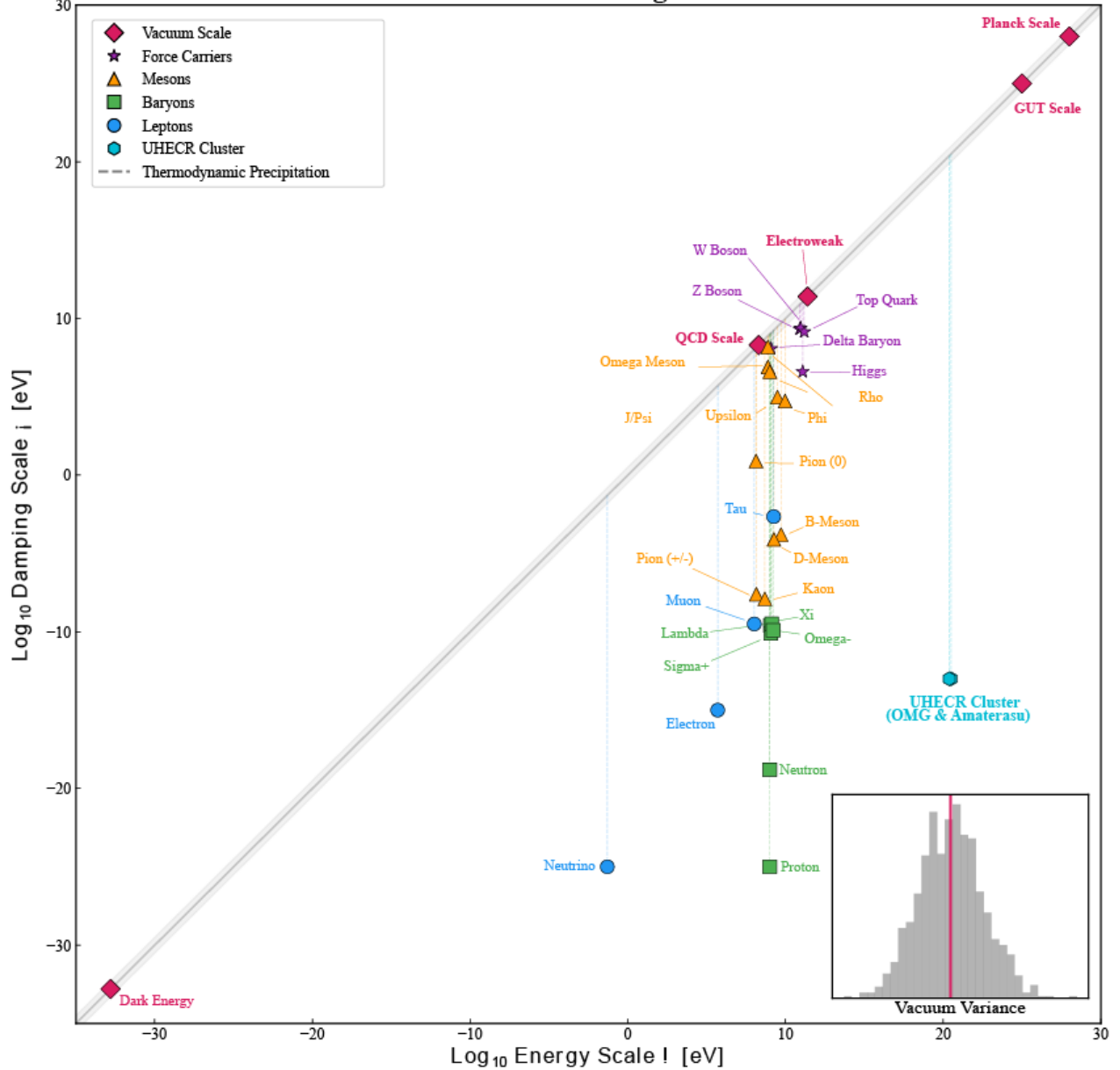


Figure 3: **Cross-scale empirical validation: stability classification across orders of magnitude.** Physical systems plotted as damping scale  $\log_{10} \Gamma$  versus characteristic frequency  $\log_{10} \omega$  from cosmological to Planck scales. **Red diamonds** indicate vacuum-lineage processes near  $\chi = \Gamma/(2\omega) \approx 1$ . **Gray arrows** illustrate schematic movement from near-critical regimes into the underdamped basin. For elementary particles,  $\omega$  is identified with rest mass (natural units) and  $\Gamma$  with the measured decay width; for effectively stable particles,  $\Gamma$  represents an upper bound or interaction-limited width at the relevant scale [16]. Particle data from PDG [16].

**Null-model comparator.** Under a null model in which  $(\omega, \Gamma)$  values are not constrained by a cross-scale organizing principle, the induced distribution of  $\chi = \Gamma/(2\omega)$  would be broadly spread in log-space rather than compressed toward a narrow neighborhood. The observed clustering of vacuum-lineage processes near  $\chi \approx 1$  and of long-lived matter at  $\chi \ll 1$  is therefore not a generic consequence of plotting conventions, but a nontrivial empirical pattern consistent with stability-based classification.

When a dominant substrate satisfies  $\chi \approx 1$ , any emergent mode with nonzero overlap inherits a component of this near-critical structure. In the dominance limit,  $|c_s|^2 \gg |c_{k \neq s}|^2$ , the emergent ratio satisfies  $\chi_\psi \rightarrow \chi_s$ . Emergent parameters are therefore constrained projections of pre-existing substrate properties rather than independent tunings. The stability landscape is schematically represented in Figure 4.

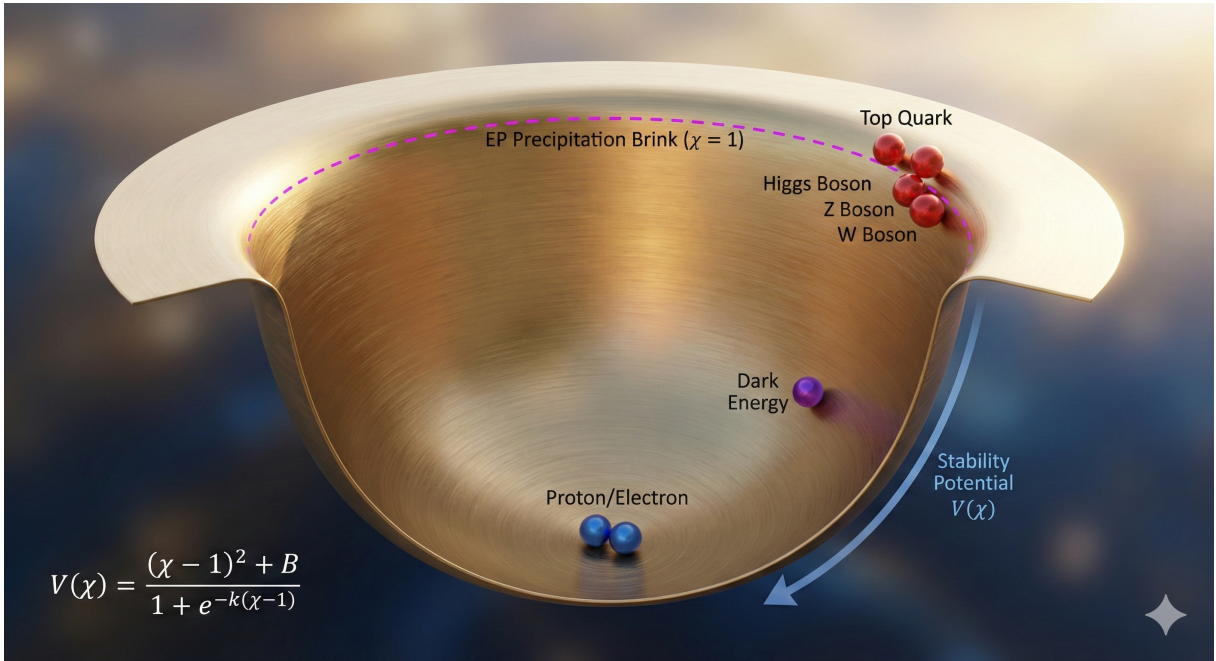


Figure 4: **Schematic stability landscape: state-space representation of the basin structure.** The revolved surface illustrates the stability hierarchy across the particle spectrum using an illustrative mapping in  $\chi$ -space. This functional form is a visualization aid, not a derived fundamental potential. The rim ( $\chi = 1$ ) denotes the exceptional-point boundary separating overdamped and underdamped solution classes. Long-lived matter occupies the basin where detuning and impedance mismatch suppress rapid decay, while broad resonances cluster near the rim where partial resonance permits rapid decay.

### 5.1 Structural Role of Gauge Couplings

Within the stability architecture, gauge couplings are classified as *substrate-ratio parameters*. In representative open-field settings, interaction-induced broadening rates admit scaling of the form  $\Gamma_i \propto g_i^2 \Omega_i$  up to model-dependent phase-space factors and kinematic thresholds, where  $\Omega_i$  denotes a characteristic sector frequency at the scale of interest. The effective stability index  $\chi_i = \Gamma_i/(2\Omega_i)$  therefore depends directly on the gauge coupling.

The persistence of a gauge sector as a coherent substrate requires operation within the near-critical window  $\chi_i \approx 1$ . This condition constrains  $g_i^2$  to values that maintain spectral balance between interaction-induced damping and coherent propagation across renormalization-group flow. In this sense, gauge couplings are not freely tunable parameters, but ratios fixed by stability consistency.

The framework does not claim a parameter-free derivation of the numerical values of  $(g_1, g_2, g_3)$ . Instead, it provides a stability-based classification: the couplings control the ratio between interaction-induced broadening and coherent sector frequency, and therefore determine whether a sector admits near-critical operation in the sense of  $\chi_i = \Gamma_i/(2\Omega_i)$ . Any stronger claim requires specifying  $(\Omega_i, \Gamma_i)$

operationally and demonstrating the mapping to the measured renormalized couplings at a fixed reference scale.

## 6 Experimental and Observational Tests

Having established the structural role of the  $\chi = 1$  boundary across quantum, field-theoretic, and cosmological dynamics, this section outlines concrete experimental and observational tests capable of confirming or falsifying the stability architecture.

The structural identity of the  $\chi = 1$  boundary yields falsifiable predictions across accessible energy scales. Each test below specifies an observable, a measurable threshold, and the conditions under which this framework would be challenged.

### 6.1 Cosmological Synchronization (DESI & Euclid)

In flat  $\Lambda$ CDM, the onset of cosmic acceleration ( $q = 0$ ) and the critical damping of structure growth ( $\chi_\delta = 1$ ) occur at the same transition redshift  $z_t$ . Extensions such as curvature or dynamical dark energy ( $w(z) \neq -1$ ) generically break this synchronization, producing an offset  $\Delta z = z_{q=0} - z_{\chi=1}$ .

- **Observable:** The redshift difference  $\Delta z$  between the kinematic transition ( $q = 0$ ) inferred from supernovae/BAO and the structural transition ( $\chi_\delta = 1$ ) inferred from growth-rate measurements ( $f\sigma_8$ ).
- **Sensitivity Requirement:** Upcoming surveys (DESI, Euclid, Rubin) are expected to constrain  $z_t \approx 0.6$  with precision  $\sigma_z < 0.05$ . A statistically significant offset  $|\Delta z| > 3\sigma_z$  that cannot be attributed to curvature or  $w(z)$  evolution would challenge the structural identity.

### 6.2 Quantum Spectral Merger (Circuit QED)

The transition from underdamped oscillation to overdamped decay at  $\chi = 1$  predicts a unique spectral signature: the coalescence of eigenfrequencies into a second-order exceptional point (EP2). This can be probed in superconducting qubit–cavity systems with tunable coupling  $g$ .

- **Protocol:** A transmon qubit ( $\omega_q/2\pi \approx 5$  GHz) coupled to a dissipative cavity ( $\kappa/2\pi \approx 1$  MHz) is tuned through the exceptional point by varying the Purcell decay rate  $\gamma_P = \kappa g^2/\Delta^2$ .
- **Signature:** As  $\chi$  is scanned through  $\{0.8, 0.9, 1.0, 1.1\}$ , the qubit population  $P_1(t)$  must transition from oscillatory decay  $e^{-\gamma t/2} \cos(\omega_a t)$  to the EP2 kernel  $t e^{-\omega t}$  at the critical point, accompanied by spectral doublet merger  $\omega_{\pm} \rightarrow \omega_0$ .
- **Sensitivity Requirement:** Time-domain sampling with  $\delta t \leq 10$  ns over a  $10\ \mu\text{s}$  window is required to resolve the critical power-law tail. A failure to observe spectral coalescence within the expected window  $0.95 < \chi < 1.05$  would challenge the existence of the EP2 boundary in open quantum dynamics.

### 6.3 Finite-Temperature QCD Coherence (Lattice)

If the QCD substrate participates in near-critical stability organization, lattice determinations of finite-temperature spectral functions should reveal a scalar ( $0^{++}$ ) channel with damping ratio  $\chi \equiv \Gamma/(2\Omega)$  approaching unity in the vicinity of the confinement transition.

- **Observable:** The thermal pole or peak location  $\Omega(T)$  and width  $\Gamma(T)$  extracted from spectral reconstructions in the  $0^{++}$  channel.

- **Signature:** Existence of a temperature band near the transition where  $0.8 \lesssim \chi(T) \lesssim 1.0$ .
- **Challenge condition:** Absence of any near-critical window in all plausible reconstruction methods would weaken the substrate-coherence interpretation.

#### 6.4 Neutron Star Ringdown (Gravitational Waves)

For neutron-star  $f$ -modes, the damping time  $\tau$  and oscillation frequency  $f$  define a dimensionless stability index  $\chi_{\text{NS}} = (2\pi f\tau)^{-1}$ . As compact objects approach the TOV limit, the mode trajectory is predicted to approach the structural boundary  $\chi_{\text{NS}} \approx 1$ .

- **Test:** Third-generation gravitational-wave detectors (Cosmic Explorer, Einstein Telescope) should observe that remnant objects populate the region  $\chi_{\text{NS}} \leq 1$ ; a statistically significant population with  $\chi_{\text{NS}} > 1$  would contradict the stability-boundary interpretation.

## 7 Conclusion

A single dimensionless ratio,  $\chi = \gamma/(2|\omega|)$ , defines a stability architecture across quantum, field-theoretic, and cosmological dynamics. The critical boundary  $\chi = 1$  marks a non-Hermitian exceptional point that coincides exactly with the onset of cosmic acceleration via the identity  $\chi_\delta = 1 \iff q = 0$ . Substrate inheritance constrains emergent parameters without invoking phenomenological tuning, and observed particle hierarchies are consistent with stability-based classification.

**Interpretation.** Any apparent preference for  $\chi \approx 1$  is interpreted as survivorship under stability constraints rather than as an optimization principle imposed by nature. In this view, the critical boundary functions as a separatrix that organizes which structures can persist, not as a target that dynamics must seek. These results establish  $\chi$  as a structural organizing principle of physical reality.

**Falsifiability.** The framework yields several independent tests. (i) In flat  $\Lambda$ CDM, the transitions  $\chi_\delta = 1$  and  $q = 0$  must coincide; any observed offset would falsify the structural identity. (ii) Finite-temperature lattice QCD must exhibit a  $0^{++}$  mode with  $\chi \approx 1$  near the confinement transition. (iii) Quantum platforms with tunable  $\gamma/\omega$  must display spectral-peak merger and the EP2 kernel at  $\chi = 1$ . (iv) Neutron-star oscillation modes should approach  $\chi_{\text{NS}} \rightarrow 1$  near the TOV limit. These tests collectively determine whether the stability architecture described here is realized in nature.

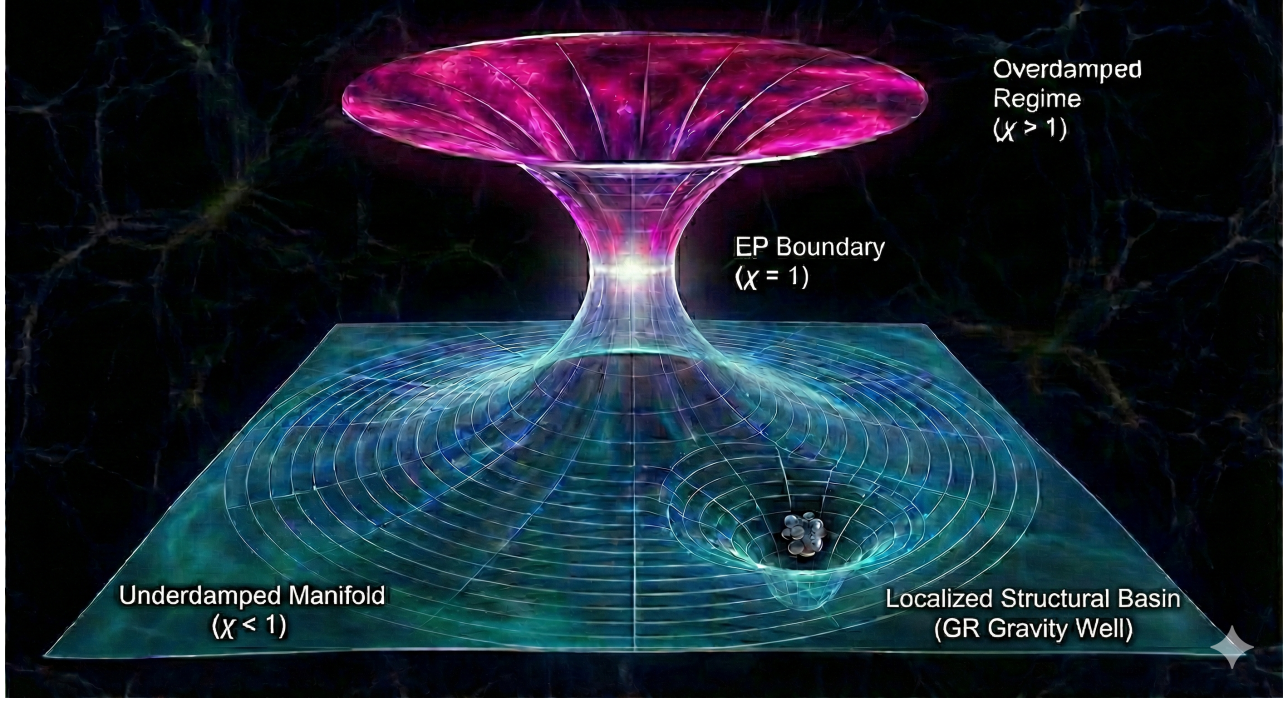


Figure 5: **Unified topology: vacuum-to-spacetime structure.** The funnel represents the stability manifold in  $\chi$ -space, separating overdamped ( $\chi > 1$ ), exceptional ( $\chi = 1$ ), and underdamped ( $\chi < 1$ ) dynamical regimes. This is parameter space, not spatial geometry. The visualization provides a stability-theoretic correspondence with general-relativistic curvature and does not replace Einstein dynamics.

## References

- [1] Abbott, B. P., et al. (2020). GW190814: Gravitational waves from coalescence. *Astrophysical Journal Letters*, 896, L44.
- [2] Aspelmeyer, M., Kippenberg, T. J., & Marquardt, F. (2014). Cavity optomechanics. *Reviews of Modern Physics*, 86, 1391-1452.
- [3] Bender, C. M. (2007). Making sense of non-Hermitian Hamiltonians. *Reports on Progress in Physics*, 70, 947-1018.
- [4] Blais, A., et al. (2021). Circuit quantum electrodynamics. *Reviews of Modern Physics*, 93, 025005.
- [5] Breuer, H.-P., & Petruccione, F. (2002). *The Theory of Open Quantum Systems*. Oxford University Press.
- [6] Cardoso, V., Franzin, E., & Pani, P. (2016). Is the gravitational-wave ringdown a probe of the event horizon? *Physical Review Letters*, 116, 171101.
- [7] Carmichael, H. J. (1999). *Statistical Methods in Quantum Optics 1*. Springer.
- [8] Clerk, A. A., et al. (2010). Introduction to quantum noise, measurement, and amplification. *Reviews of Modern Physics*, 82, 1155-1208.

- [9] DESI Collaboration. (2024). DESI 2024 VI: Cosmological constraints from BAO. arXiv:2404.03002.
- [10] Dodelson, S. (2003). *Modern Cosmology*. Academic Press.
- [11] Gorini, V., Kossakowski, A., & Sudarshan, E. C. G. (1976). Completely positive dynamical semigroups of N-level systems. *Journal of Mathematical Physics*, 17, 821-825.
- [12] Heiss, W. D. (2012). The physics of exceptional points. *Journal of Physics A: Mathematical and Theoretical*, 45, 444016.
- [13] Kato, T. (1995). *Perturbation Theory for Linear Operators*. Springer.
- [14] Lindblad, G. (1976). On the generators of quantum dynamical semigroups. *Communications in Mathematical Physics*, 48, 119-130.
- [15] Ogata, K. (2010). *Modern Control Engineering* (5th ed.). Prentice Hall.
- [16] Particle Data Group. (2022). Review of particle physics. *Progress of Theoretical and Experimental Physics*, 2022, 083C01.
- [17] Peebles, P. J. E. (1993). *Principles of Physical Cosmology*. Princeton University Press.
- [18] Perlmutter, S., et al. (1999). Measurements of  $\Omega$  and  $\Lambda$  from 42 high-redshift supernovae. *Astrophysical Journal*, 517, 565-586.
- [19] Planck Collaboration. (2020). Planck 2018 results. VI. Cosmological parameters. *Astronomy & Astrophysics*, 641, A6.
- [20] Riess, A. G., et al. (1998). Observational evidence from supernovae for an accelerating universe. *Astronomical Journal*, 116, 1009-1038.
- [21] Wilson, K. G., & Kogut, J. (1974). The renormalization group and the  $\epsilon$  expansion. *Physics Reports*, 12, 75-199.
- [22] Christensen, N. (2026). The Primordial Boundary Principle: Identifying Cosmic Acceleration with Exceptional Point Coalescence. *Zenodo*. <https://doi.org/10.5281/zenodo.17490497>
- [23] Christensen, N. (2026). Structural Mapping of Linear Damping Operators Across Cosmological Growth and Black Hole Ringdown. *Zenodo*. <https://doi.org/10.5281/zenodo.17503537>
- [24] Christensen, N. (2026). Structural Constraints from Critical Damping in Open Quantum Field Theories: Implications for QCD Substrate Inheritance and Phenomenological Extensions. *Zenodo*. <https://doi.org/10.5281/zenodo.17437688>
- [25] Christensen, N. (2026). Density-Dependent Matter-Induced Dephasing in Neutrino Oscillations with Preserved Vacuum Unitarity . *Zenodo*. <https://doi.org/10.5281/zenodo.17585527>
- [26] Christensen, N. (2026). Closing Critical Gaps: Physical Inheritance from Stabilized Substrates in Dynamical Systems. *Zenodo*. <https://doi.org/10.5281/zenodo.17428940>